URTeC: 3724108

Using Quantitative Tracer Analysis to Calibrate Hydraulic Fracture and Reservoir Simulation Models: A Permian Basin Case Study

Magdalene Albrecht*[1], Shannon Borchardt[1], Chase Murphree[1], Mark McClure[2], Janz Rondon[2] 1. SM Energy, 2. ResFrac Corporation.

Abstract

Well spacing and hydraulic fracture design optimization are among the most important challenges confronting companies operating in unconventional reservoirs. Field trials are time consuming and expensive. Reservoir simulation and/or rate transient analysis can help guide development decisions, but these calculations can be affected by non-uniqueness. For example, it is not possible to resolve permeability and fracture geometry using only production and pressure data in rate transient analysis. This work demonstrates that tracers can be used to reduce non-uniqueness. We quantitatively apply tracer measurements as part of the calibration and history matching of a fully coupled 3D hydraulic fracturing, geomechanics, and reservoir simulator. With the use of calibrated models, forward modeling and sensitivity analysis can be used more accurately to guide better decisions about well spacing and hydraulic fracture design. Tracers are complementary to data sources such as microseismic and distributed acoustic sensing, which focus on hydraulic fracture creation but provide less constraint on the producing behavior of wells, which ultimately drives asset financial performance.

Introduction

Operators in unconventional oil and gas reservoirs utilize a variety of economic metrics to guide investment decisions, including: net present value, rate of return, and capital efficiency. Horizontal wells and their completion comprise a large portion of an operator's capital spend. Thus, it is critical to optimize this spend.

Fig. 1 depicts a theoretical well spacing sensitivity. There are numerous choices an operator can make regarding the completion of a well, including: stage spacing, cluster spacing, perforation configuration, fluid intensity, and proppant loading. This quickly becomes a complex problem when trying to link the cost of changing these parameters to the design objective, as depicted in the plot of net present value (NPV) vs. estimated ultimate recovery (EUR).

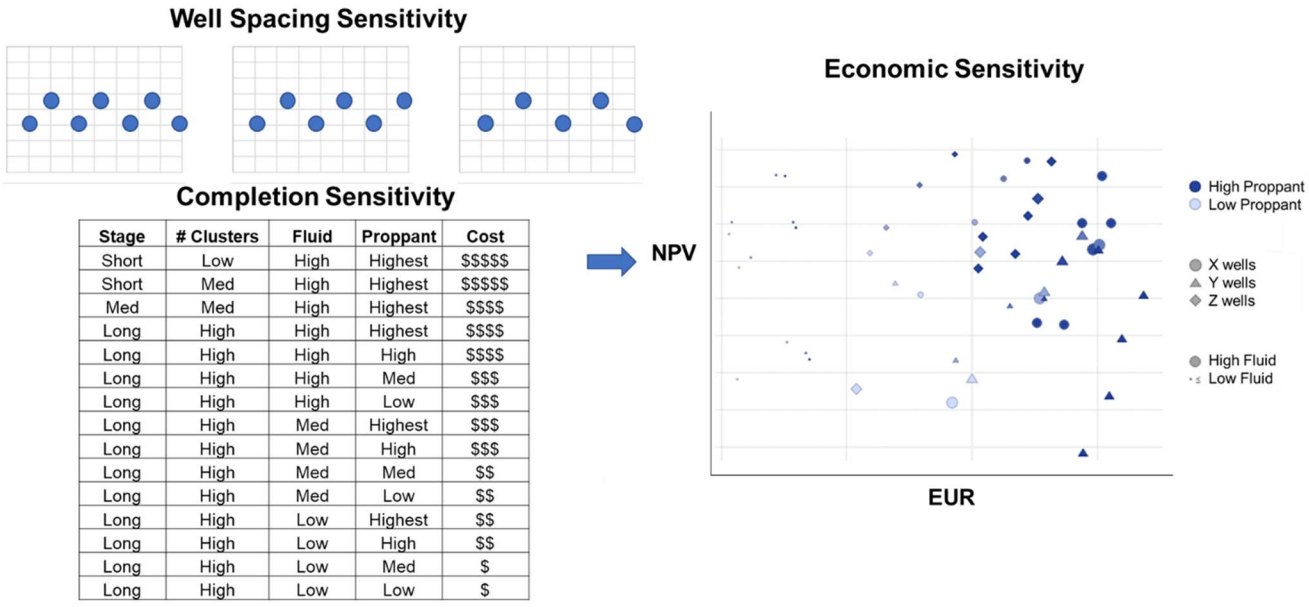

Stage	# Clusters	Fluid	Proppant	Cost
Short	Low	High	Highest	$$$$$
Short	Med	High	Highest	$$$$$
Med	Med	High	Highest	$$$$
Long	High	High	Highest	$$$$
Long	High	High	High	$$$$
Long	High	High	Med	$$$
Long	High	High	Low	$$$
Long	High	Med	Highest	$$$
Long	High	Med	High	$$$
Long	High	Med	Med	$$
Long	High	Med	Low	$$
Long	High	Low	Highest	$$
Long	High	Low	High	$$
Long	High	Low	Med	$
Long	High	Low	Low	$

Fig. 1—A hypothetical well spacing, completion, and economic sensitivity.

To perform a sensitivity analysis like the one depicted in Fig. 1, operators often use numerical simulators. However, it can sometimes be challenging to validate their underlying inputs. Non-uniqueness is particularly problematic in ultra-low permeability reservoirs because the time between diagnostic flow regimes exceeds the short window needed for investment decisions. This is especially true if the history matched model is constrained solely by bottomhole pressures and oil/water/gas rates. Simulation models matched solely to production data may yield orders of magnitude differences in permeability and may be matched with different conceptual models such as stimulated rock volume (SRV). Resulting path-forward models may result in major differences regarding critical development recommendations around well spacing and completion design (Fowler et al. 2019).

Field diagnostics make it possible to decrease the non-uniqueness in the production history match. Microseismic has been utilized for several decades to understand hydraulic fracture geometry in unconventional plays. Distributed acoustic sensing (DAS) and sealed wellbore pressure monitoring (SWPM) have gained popularity in recent years because they provide direct observations from offset wells to understand the timing of fracture propagation relative to completion volumes pumped. However, these diagnostic tools are limited to characterizing the generation of hydraulic fractures, and do not measure the effectively draining fracture length.

Thus, it is valuable to use diagnostic tools that better constrain the producing time period. Such tools include downhole pressure gauges, interference testing, permeability estimates from interpretation of diagnostic fracture injection tests (DFITs) and core testing, geochemical production allocation, and chemical tracers.

This paper focuses on conservative, phase-specific tracers. Tracer studies provide low-cost diagnostics that can be easily analyzed in a spreadsheet. We use case studies in the Permian Basin to demonstrate how tracers provide a valuable spatial and temporal constraint for the history matching of hydraulically fractured wells. A companion paper by Albrecht et al. (2022) discusses how geochemical production allocation provides additional spatial and temporal constraint on productive fracture area.

Theory and Methods

Tracers are a well-established technology used to characterize both conventional hydrocarbon and geothermal reservoirs. Tracers have been used for over 60 years to characterize waterflood patterns (Brigham and Smith 1965) and have been incorporated into conventional reservoir simulation models (Ali et al. 2000; Gaibor and Rodriguez 2015). These conventional applications have focused on efforts to understand inter-well communication, with an emphasis on both use of water phase tracers and qualitative over quantitative interpretations (Du and Guan 2005).

Quantitative tracer analysis is based on residence time calculations, or first moment analysis, as described by Danckwerts (1953) in the application of packed bed reactors. The relevant equations discussed in a geothermal case study shared by Shook (2005) are used to normalize tracer production data into the age distribution function in **Eq. 1**.

$$E(t)_{Actual} = \frac{C(t)\rho\, q}{M}, \text{units of } \frac{1}{days}$$

$C(t)$ = Concentration of tracer over time
ρ = Density of soluble phase
q = Flow rate of soluble phase
M = Mass of injected tracer

(1)

Eq. 1 is applicable to conventional reservoirs (such as in 5-spot water flood patterns), geothermal reservoirs (producer-injector pairs), and unconventional well injection and production.

Quantitative tracer analysis requires that tracers are conservative from a mass balance perspective. Conservative is defined in both field applications and simulation models as not reactive with downhole fluids, not adsorbing to surfaces, and not partitioning to other phases. It is also assumed that the flowing properties of the tracer, such as density and viscosity, can be specified in terms of the phases of interest, typically water, oil, or gas. Ideal conservative tracers also are not naturally occurring in the reservoir system. Tracers may be injected into a well as a slug/pulse, injected continuously, or injected and recycled via produced water. Further discussion on the topic of ideal tracers is found in papers by Shook et al. (2004, 2009).

For the purposes discussed in this paper, the authors will focus on tracers as they are typically deployed in unconventional oil and gas reservoirs. In unconventional plays, a known mass of fluid tracer is continuously injected throughout one or more stages. Total tracer mass is typically on the order of a pound of tracer injected per thousand barrels of water. Upon well startup, the production streams of the well with injected tracers are sampled at surface. Offset wells may also be sampled. An example is shown in **Fig. 2**, with hydraulic fractures shown in red and a cross section along the wellbores of the matrix cells in blue.

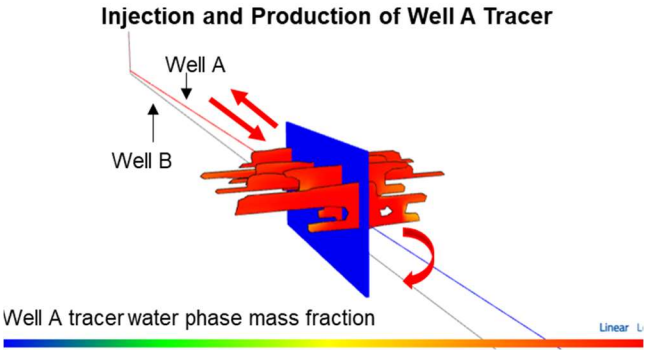

Fig. 2—Tracer injected into Well A, produced from Well A and Well B.

A laboratory then analyzes the samples and reports concentration of the tracer found in the carrier phase. Examples of raw data outputs for six unique tracers are shown in **Table 1**.

Tracer Injected (g)	1681	1657	1634	829	876	781
% Injected	3%	3%	3%	2%	2%	2%
Sample Date	CFT 10450	CFT 3900	CFT 10750	CFT 4800	CFT 10350	CFT 10300
10/17/16 15:00	5.8	1.3	1.9	1.5	1.3	1.8
10/18/16 5:00	7.1	1.3	2.5	1.7	1.8	1.8
10/18/16 17:00	6.8	1.7	2.3	1.8	1.9	1.8
10/19/16 5:00	5.5	2.0	2.2	2.0	2.3	1.8
10/20/16 5:00	5.8	1.8	2.0	2.0	2.2	1.7
10/21/16 5:00	6.5	1.6	2.1	2.2	2.6	1.8

Table 1—An example of laboratory reported tracer concentrations and amount injected.

Table 1 contains both the mass of tracer M and the concentration of tracer with respect to time C(t) found in Eq. 1. To make use of quantitative tracer analysis, we must combine the provided data with relevant phase production data, density, and appropriate unit conversions. For the remainder of this paper, the age distribution function E(t) in Eq. 1 will be referred to as tracer recovery rate. Integrating Eq. 1 results in cumulative tracer recovery shown in **Eq. 2**, expressed as a fraction or percent of the total tracer initially injected.

$$\text{Cumulative Tracer Recovery} = \int E(t)_{Actual}\text{dt} \tag{2}$$

Application of Eqs. 1 and 2 to both actual tracer data and simulation models provides a way to compare results over time. The challenge with incorporating tracer data into simulation models in low-permeability reservoirs is that this requires modeling both injection and production of the tracers, spatially and temporally. Historically, this has not been possible because subsurface workflows focus on fracture modeling separate from modeling the production system. To model tracers correctly in a standard reservoir simulator alone, a simulation engineer would need to initialize a model knowing where tracer is present prior to the start of production, as well as the conductivity of the fractures and propped area containing tracers.

To address this challenge, a fully coupled hydraulic fracture, geomechanics, and 3D reservoir simulator was used to examine the datasets shared in these case studies (McClure et al. 2022). This single simulator package honors the mass balance of tracer by both tracking its injection into and production from the reservoir/fracture/well system located within the model boundaries. The propped and unpropped fracture area making up the fracture mesh portion of the model is determined by the fracturing simulator. In the simulations described in this paper, each fracture element generated by the injected completion is on the order of 120 by 120 ft^2, which was chosen to balance runtime with accuracy for eventual use in multi-well

model sensitivities. To improve accuracy and handle thin beds, the MuLTipEl algorithm from Dontsov et al. (2022) is used to submesh the elements.

The growth of hydraulic fractures and subsequent fluid production is dependent on many subsurface variables, including: porosity, saturation, permeability, relative permeability, elastic properties, pore pressure, earth stresses, toughness, layering, interfaces, discontinuities, etc. A simulation model was built incorporating some of these parameters. Most of the properties were estimated from log measurements calibrated to core samples. The static model was created from log derived properties and then upscaled to a resolution appropriate for reservoir simulation using similarities and differences in petrophysical and geomechanical log properties.

While the growth and propagation of hydraulic fractures in the subsurface is complicated and influenced by many parameters, a reasonable representation is possible with a good understanding of leakoff, elastic properties, earth stresses, and fracture toughness. In the case studies that will be discussed, leakoff, elastic properties and earth stresses were reasonably well constrained. Leakoff was estimated from an understanding of permeability and relative permeability measured by logs and core. Elastic properties such as Young's Modulus and Poisson's Ratio were measured with sonic logs and calibrated to static core measurements, considering transverse anisotropy. Minimum horizontal stress was estimated continuously using sonic logs accounting for transverse anisotropy and calibrated to measurements of closure from DFITs taken in multiple formations in offset horizontal wells. This allowed for a continuous estimate of calibrated minimum horizontal stress vertically throughout the formations intersected by the hydraulic fracture. One parameter that was not well constrained, which required iterations in the simulation, was fracture toughness. Toughness was varied as part of the calibration process to match actual tracer data over time. Toughness is used as a model fitting parameter because it is known to be scale-dependent, but this scale-dependence is formation-specific and difficult to predict in advance.

For all modeled wells within the case study areas, actual well depths and trajectories, perforation clusters, completion fluids, and proppant properties were honored. One completion stage per well was modeled, honoring injection rates, volumes, and proppant ramps used in the field to generate hydraulic fractures. Production rates in the model were controlled using an estimate of each well's flowing bottom hole pressure, calculated using tubing flow correlations from downhole gauges and/or surface pressure and wellbore casing and tubing configurations.

History matching is accomplished by using flowing bottom hole pressure to match each well's actual production volumes of oil, gas and water with the simulator outputs. The simulations include only one or a few stages along each well; for history matching, the production volumes are scaled proportionally with the total number of completion stages. We assume that over time, the individual completion stage contributions are equal along the length of a completed horizontal wellbore.

The generation of simulation results comparable to tracer diagnostic data begins with the definition of the tracers within the model. The tracers are assumed to be inert and have no impact on the properties of the carrier phase. It was assumed that the tracers have a molecular weight below that of a weight in which a filter cake develops, consistent with the weight of commonly used tracers such as perfluorobenzoic acids (Shook et al. 2009).

Fig. 3 depicts how injecting a tracer laden fluid type results in both the creation of hydraulic fractures and transport of the tracer laden fluid through the hydraulic fractures. Water tracers are injected into one well in a two well vertical stack scenario. Only fractures generated by Well A in red and a cross section of the simulation matrix cells along the completion stage in blue are shown. The left side of Fig. 3 shows water phase mass fraction of a unique tracer injected into Well A at the beginning of the injection sequence, and the right side shows the same view at the end of the injection sequence.

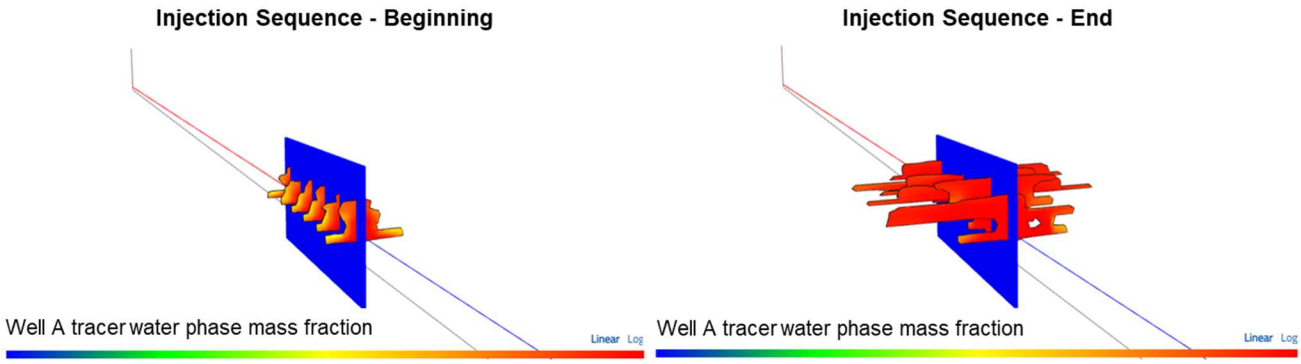

Fig. 3—Sequence of tracer injection at the beginning and end of a single stage completion.

After tracer has been injected and a well has started production, Eqs. 1 and 2 can be applied to both the actual and modeled dataset. **Fig. 4** shows an example of actual and modeled well data with quantitative tracer analysis applied.

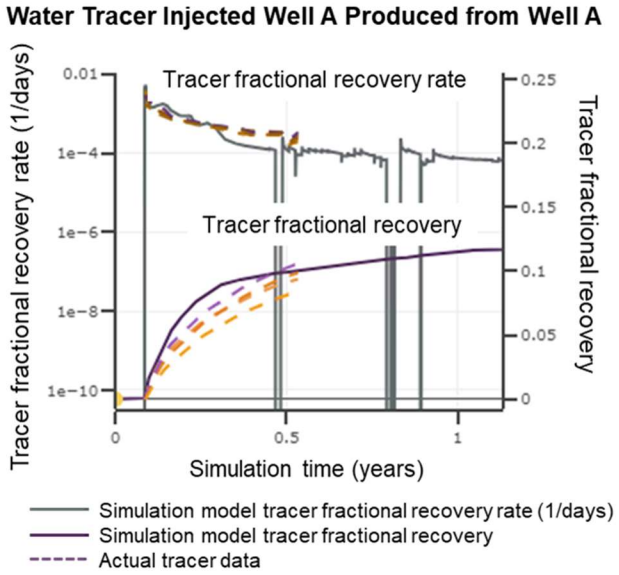

Fig. 4—Tracer fractional recovery rate and fractional recovery.

The left y-axis contains the calculations of Eq. 1 focusing on tracer recovery rate. Tracer recovery rate is plotted on a logarithmic scale in units of 1/days and includes the data located in the top of Fig. 4. The right y-axis contains the calculations of Eq. 2 focusing on overall tracer recovery which is unitless and includes the data in the bottom portion of Fig. 4. Modeled data is plotted using solid lines and actual tracer data is plotted using dashed lines. Multiple unique tracers injected into a well yields multiple dashed lines of actual tracer data that can be compared to a single modeled stage. All data shared in the case studies within this paper are shared in this format.

It is critical to look at both tracer recovery rate and calculated cumulative tracer recovery. Tracer recovery can only be calculated correctly if early time production samples are taken with sufficient frequency when tracer concentrations are rapidly changing. Tracer studies, especially those capturing parent/child effects, may not have high resolution early time data and may also contain gaps in sampling. While not ideal, the tracer recovery rate data can still be used effectively for model calibration in the absence of complete sampling history.

Case studies include multiple wells with tracer injected, and additional wells that produce tracer. **Eqs. 3 and 4** denote the constraints placed on a model with and without tracers with respect to the number of wells included.

Model Constraints without Tracers

= Number of wells (N) x Number of streams (3)
= 3N model constraints (3)

Model Constraints with Tracers

= Number of wells (N) x (Number of streams (3) + Number of tracers (T))
= N x (3 + T)
= 3N + NT model constraints (4)

In simulation models controlled by pressure, a two well scenario without tracers has six constraints with respect to time. That same two well scenario including injection of unique oil and water tracers into each well for a total of four tracers provides 14 total history matching constraints with respect to time, a considerable increase.

Fig. 5 depicts how the model solution space of all potential model inputs is reduced by the inclusion of the additional constraints. Models constrained with available production data make up a smaller population than models that do not honor the production data accurately. Yet models that accurately capture tracer diagnostic data represent an even smaller solution space than those that do not incorporate this data. This results in models that are better constrained serving as the starting point for well spacing and completion design sensitivities.

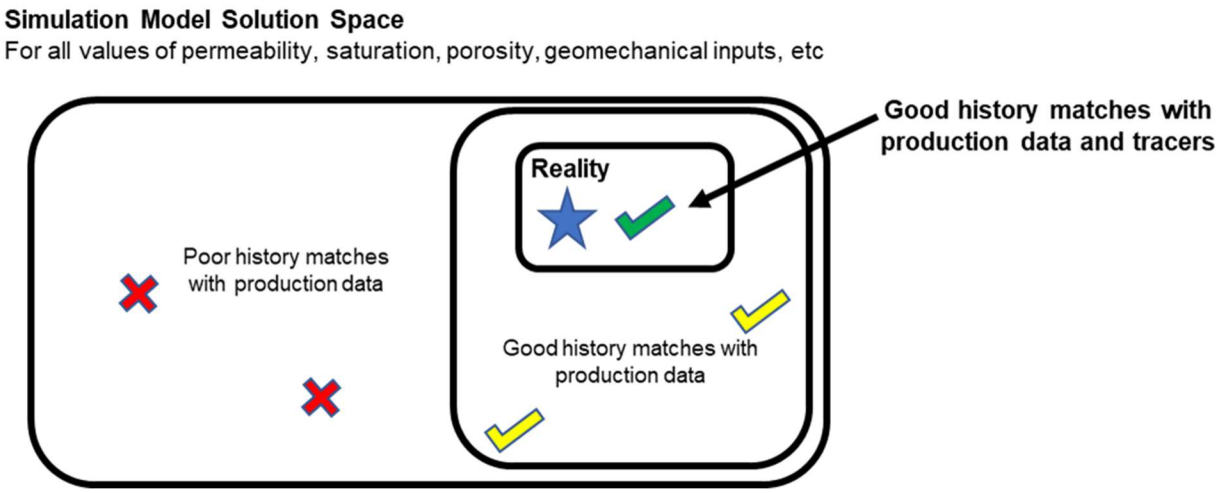

Fig. 5—Depiction of model solution space with and without incorporation of quantitative tracer analysis.

While the case studies discussed within this paper emphasize implementation and comparison using water tracers, the principles and equations are also applicable to the use of gas and oil tracers. Only the first case study will discuss use of both oil and water phase tracers.

Case Studies

The wells in these Midland Basin case studies are in two operating regions (**Fig. 6**) and target the Wolfcamp and Spraberry formations.

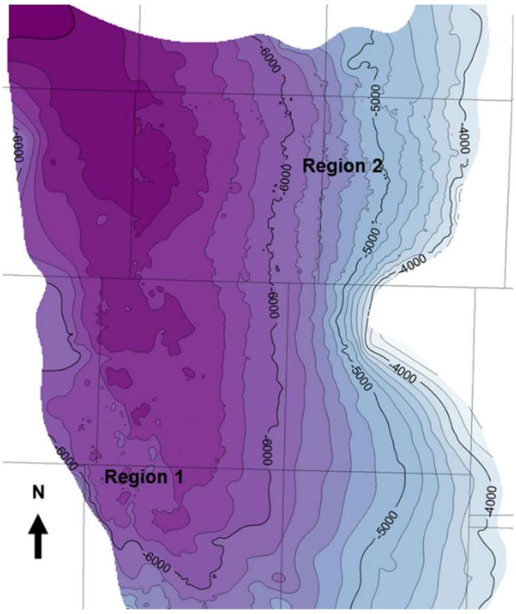

Fig. 6—Upper Wolfcamp structure map, Midland Basin.

Case Study I: Vertical Communication

The first case study uses tracer data and simulation models from Region 2. Unique oil and water tracers were continuously injected during the completion of Well A and Well B depicted in **Fig. 7** below. A unique tracer was used every one to four completion stages along the entire lateral length of both wells. Oil and water samples were taken from both wells during the first six months of production, with high frequency samples captured at well startup.

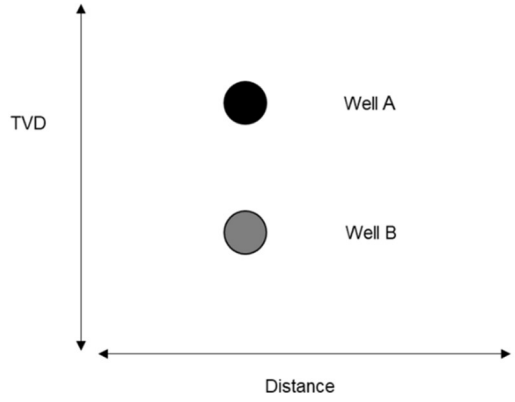

Fig. 7—Well spacing configuration of Case Study I, Region 2.

A simulation model was built of the well configuration shown in Fig. 7. Two unique water tracers and two unique oil tracers were defined within the model for each well and injected throughout the duration of the injection schedule in the model, excluding the injection of flush water volumes. The production from the modeled wells was controlled using flowing bottom hole pressure from actual downhole gauge data. Tracer rate and recovery from each well were output from the model.

Most of the subsurface properties used in the reservoir simulation were reasonably well constrained through measurements from well logs, core and DFITs. However, fracture toughness was not well constrained. In this example, history matching with the tracer response was used to help constrain the vertical toughness parameter. An original vertical toughness was used and then a sensitivity was completed by lowering the original toughness to 2/3 and 1/3 of the original value, as shown in **Fig. 8**.

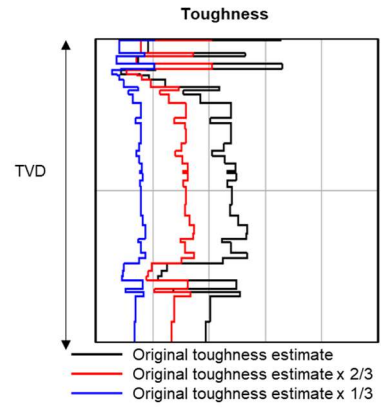

Fig. 8—Log containing three different toughness inputs for simulation model sensitivities.

A sensitivity of the model with respect to these toughness values is shown below in **Fig. 9**, where toughness was lowered from an initial assumption resulting in longer half lengths.

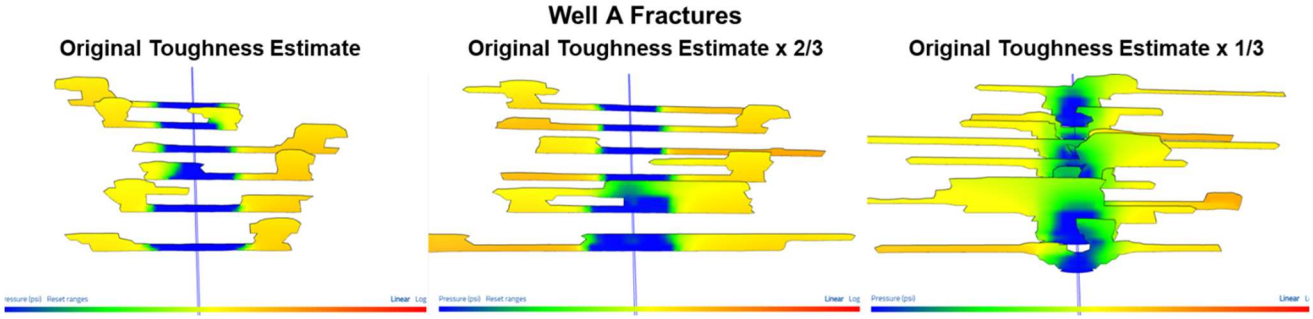

Fig. 9—Resulting hydraulic fractures from three different toughness inputs in the simulation model.

Fig. 9 shows the resulting model hydraulic fracture pressure during a time in the producing phase with respect to a sensitivity changing toughness. No matrix cells are visualized to allow for understanding fracture growth. The original toughness estimate resulted in modeled fractures with a smaller half-length and height growth than estimates at 2/3 and 1/3 of the original estimated values. The model at 2/3 of the original estimate had less height growth than the model using 1/3 the original estimated toughness and similar overall half-length. Furthermore, the modeled hydraulic fracture lengths using 1/3 original estimated toughness were corroborated by the observed distances at which increases in water production occur due to offset well completion.

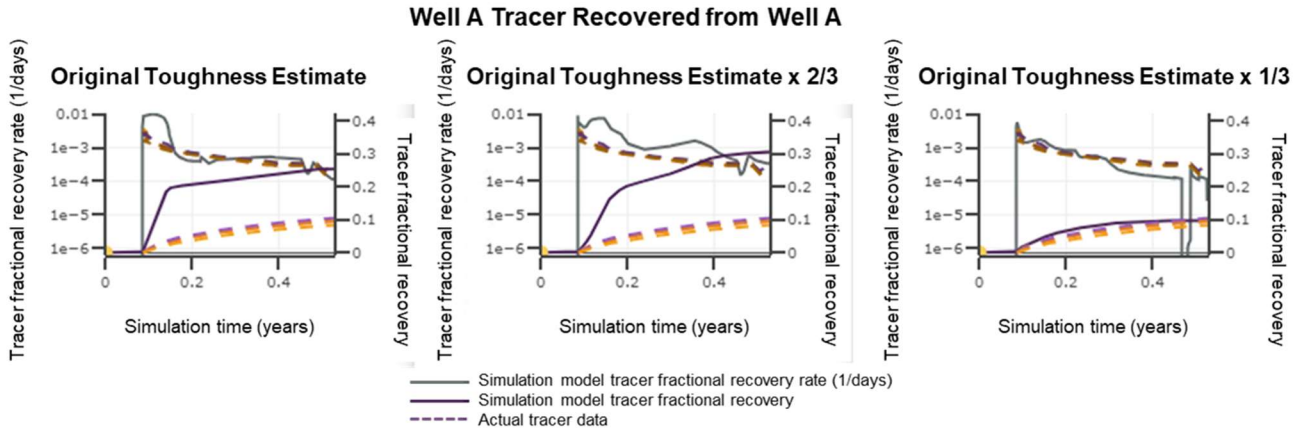

Fig. 10—Resulting modeled tracer recovery rates and tracer recovery for three different toughness inputs in the simulation model, compared with actual tracer data.

Fig. 10 shows the actual and modeled tracer recovery rate and cumulative recovery of tracer injected into and produced from Well A. The original and 2/3 original toughness estimates result in tracer recovery rate and cumulative tracer recovery that are significantly higher than observed in the actual data, as shown by the mismatch between the solid (modeled) and dashed (actual) lines in the bottom of Fig. 10. The 1/3 original toughness estimate shows a better match between modeled and actual tracer recovery.

This well stacking configuration allowed for a better understanding of vertical communication between these two wells by providing eight additional history matching parameters. These additional parameters are outlined in **Table 2** and included on the plots shown in **Fig. 11**.

	Additional History Matching Parameters
1	Water tracer injected into Well A, produced from Well A
2	Water tracer injected into Well A, produced from Well B
3	Water tracer injected into Well B, produced from Well B
4	Water tracer injected into Well B, produced from Well A
5	Oil tracer injected into Well A, produced from Well A
6	Oil tracer injected into Well A, produced from Well B
7	Oil tracer injected into Well B, produced from Well B
8	Oil tracer injected into Well B, produced from Well A

Table 2—History matching parameters for a two-well, four-tracer scenario.

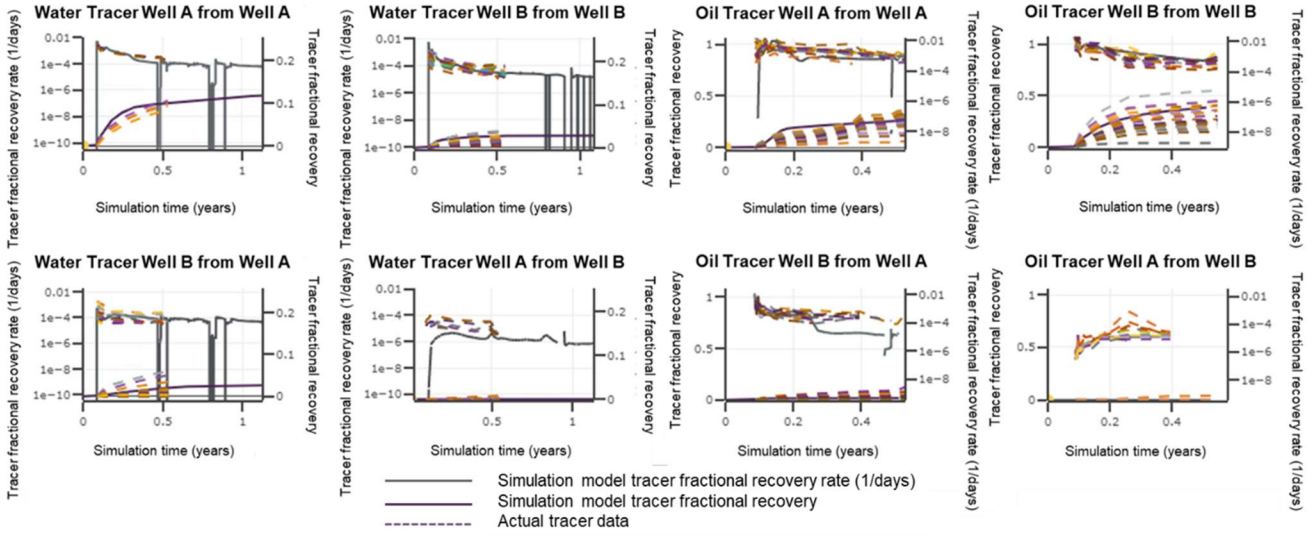

Fig. 11—Eight additional history matching parameters for a two well, four tracer scenario, Case Study I, Region 2.

Sampling of tracer was conducted over the first six months of production. During that time Well A recovered 10% of its own water tracer. The slope of fractional recovery is positive, suggesting that additional tracer would continue to be recovered had sampling for measurement of tracer in Well A continued. During the same six-month period, Well B recovered less than 5% of its own water tracer, half of what Well A was able to recover of Well A tracer despite similar completion methods. Yet 5% of Well B's water tracer was recovered from Well A located directly above Well B, suggesting vertical growth of Well B's hydraulic fractures up into the landing zone of Well A.

Fig. 12 contains a profile view of Well A and Well B fractures and horizontal wellbores with respect to the injection of Well B tracer.

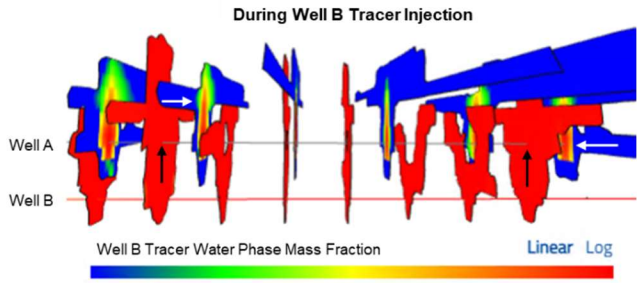

Fig. 12—Injection of tracer into Well B, hydraulic fracture crossed Well A and formed a hydraulic connection.

The blue fractures (corresponding to lower concentration of Well B tracer) were created by Well A, are located shallower, and were completed first. Red fractures indicate initiation from Well B and contain Well B water tracer. The black arrows show Well B hydraulic fracture growth up and crossing the horizontal wellbore of Well A. A setting in the simulator allows for these fractures to communicate with the wellbore, effectively modeling incomplete isolation of cement. The mechanism of tracer transport from Well B to Well A is through these hydraulic fractures that cross the wellbore. From the wellbore, the tracer can then enter the Well A hydraulic fractures, indicated by the white arrows.

Case Study II: Parent/Child and Near and Far Field Communication

The second case study also focuses on wells in Region 2. This case study was designed to understand lateral and vertical fracture propagation within a parent/child system.

One of the questions surrounding tracer transport is if tracers primarily flow along faults or hydraulic fractures. Seismic data was used to guide an interpretation of the presence of faults. Tracer was injected into completion stages away from all identified faults to focus on understanding transport within the hydraulic fracture system.

Fig. 13 contains the gun barrel well layout of Case Study II.

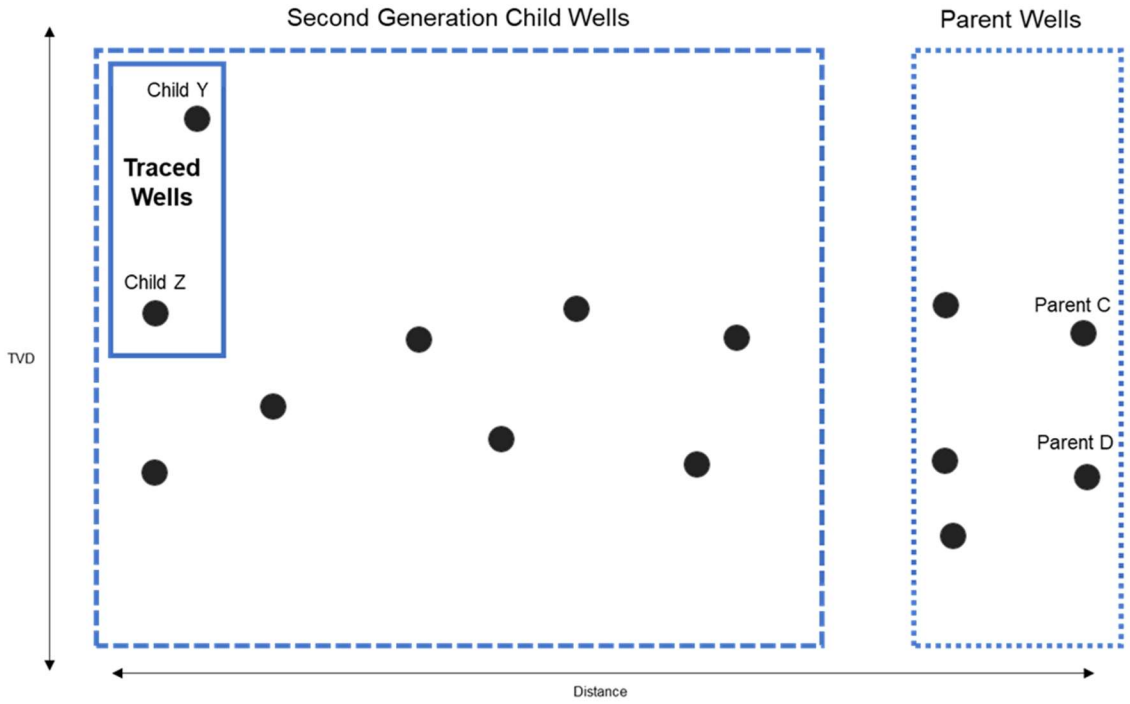

Fig. 13—Well layout of parent and child wells in Case Study II, Region 2.

Parent C, Parent D and three additional wells were completed and produced for 2 years prior to the infilling of the second-generation child wells to the west. The eastern child wells were completed first while the parent wells were shut in. Child Y and Child Z each had five unique oil and water tracers injected across a total of 15 stages. Production restarted on Parent C and Parent D during the completion of Child Y and Child Z, allowing for the opportunity to recover tracer during child well tracer injection. The three additional parent wells remained shut in.

A 14 well simulation model was built to capture this observed lateral communication. This model included the history matched static model properties from Case Study I, including the learnings on toughness.

Child Y interacted with both Parent C and Parent D wells to the east, as well as with Child Z landed directly beneath in a deeper formation. While the ratio of horizontal to vertical toughness was established in Case Study I, it was not known if these values would result in honoring far-field tracer diagnostics in a parent/child setting with wells spaced further away. Because of this uncertainty, a sensitivity on the ratio of horizontal to vertical toughness (h/v) was performed with respect to the tracer data produced from both parent and child wells.

Fig. 14 shows the resulting fracture geometry of all wells in the 14 well parent/child model using two different ratios of toughness and viewing the property of Child Y tracer at a given time. The left side contains the model using the original ratio h/v, referred to as T, assumed between horizontal and vertical toughness in Case Study I. The right side contains the resulting fractures using a ratio of T/2, achieved via increasing the vertical toughness. Note the reduction in this ratio resulted in longer overall fracture length as measured by the black arrows in the right side of Fig. 14.

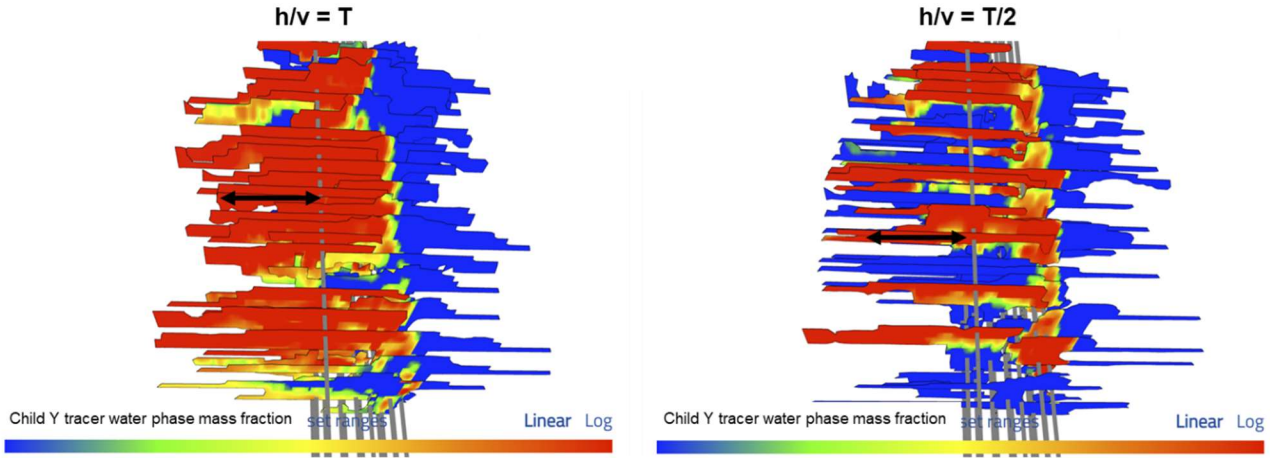

Fig. 14—Hydraulic fractures showing Child Y tracer water phase mass fraction for two different ratios of modeled toughness inputs.

Fig. 15 shows the results of tracer recovery rate and recovery of tracer injected into Child Y and recovered in Parent D for the above two models using ratios of T and T/2 for h/v toughness. Note the order of magnitude mismatch in tracer recovery rate and excessive tracer recovery in the model using T/2 with laterally longer, vertically shorter fractures.

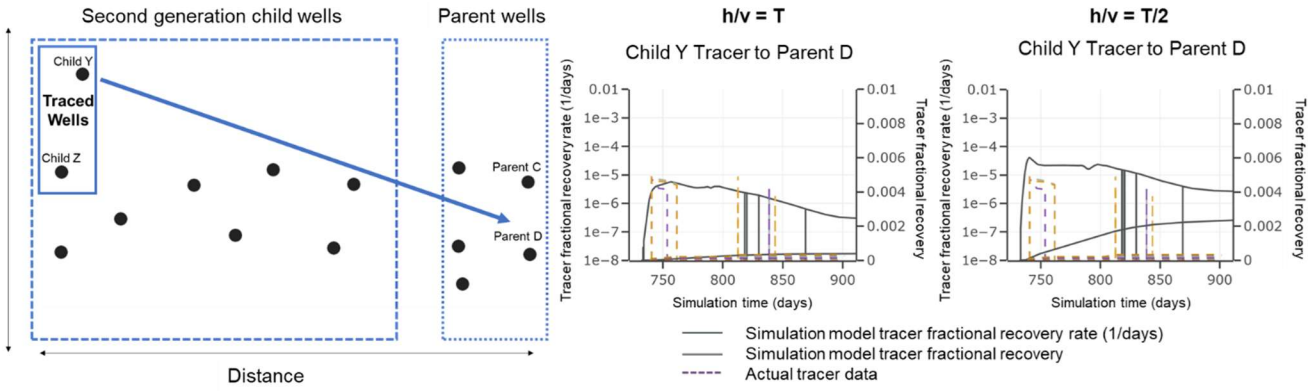

Fig. 15—Fractional rate and recovery of Child Y water tracer from Parent D.

The results focused on the near field communication between Child Y and Child Z with respect to this toughness sensitivity are shared next. **Fig. 16** is a side view comparison between the resulting fractures of Child Y and Child Z with respect to the h/v toughness ratio, with a cross section of the simulation matrix cells shown in gray. The original ratio results in hydraulic fractures in both landing zones with more height growth and overlap compared to the T/2 ratio.

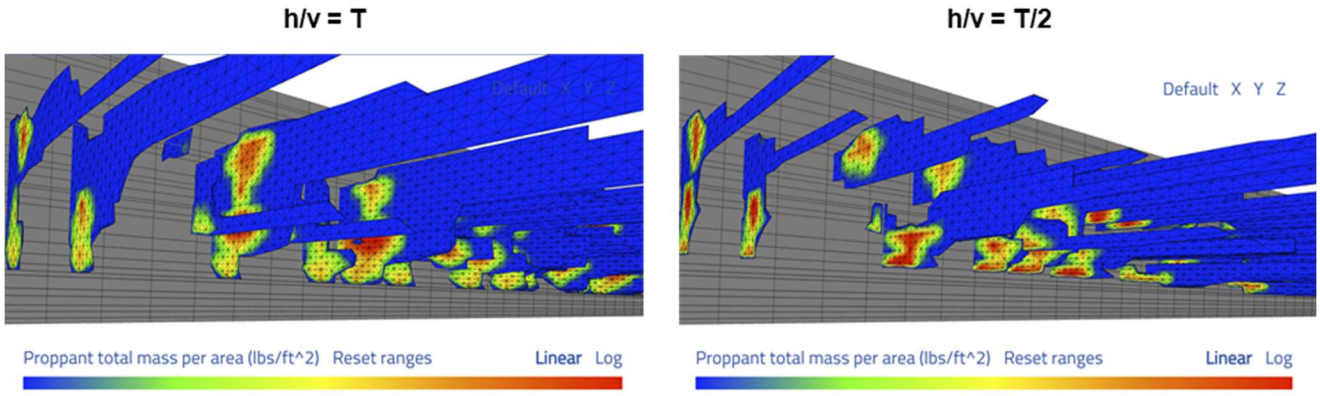

Fig. 16—Differences in modeled hydraulic fracture height and length by varying input toughness ratio.

The corresponding tracer recovery rate and tracer recovery of Child Z water tracer from Child Y and Child Y water tracer from Child Z with respect to the toughness ratio sensitivity are shown in **Fig. 17**. The original ratio more closely captures both Child Y and Child Z tracer recovery due to the increased height of the resulting fractures as compared to the halved toughness ratio and vertically shorter modeled fractures.

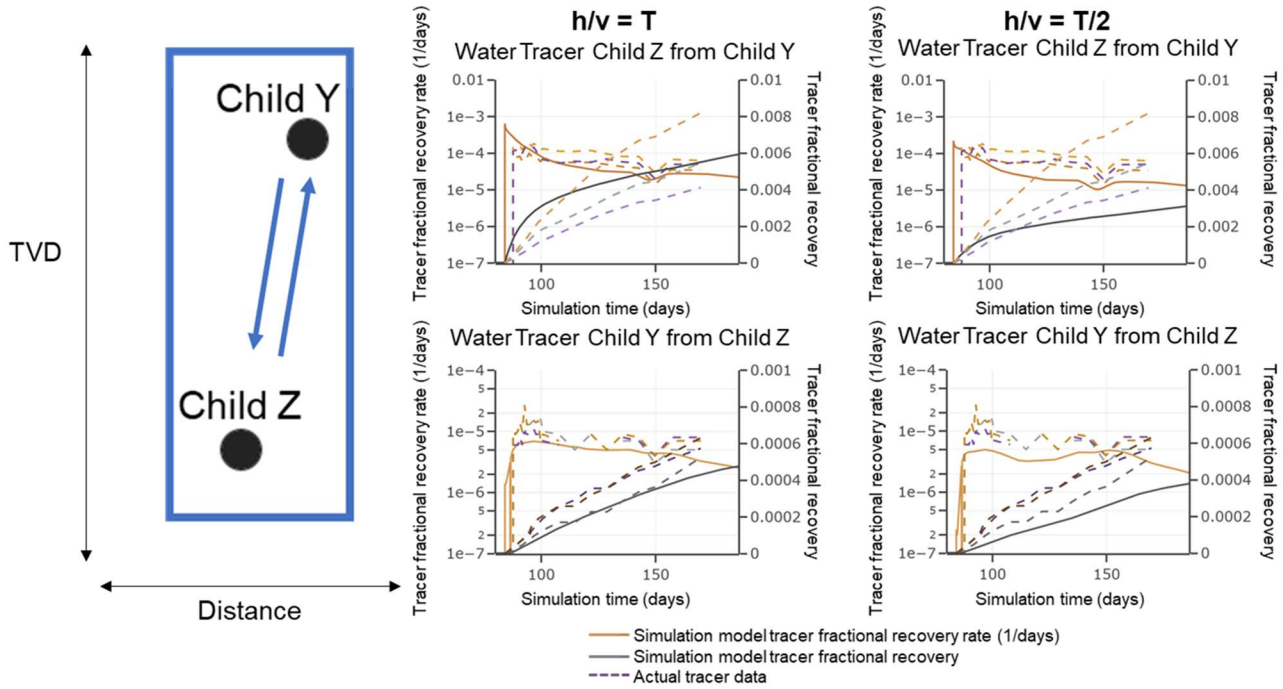

Fig. 17—Differences in modeled tracer recoveries between Child Y and Z as a result of changing the input toughness ratio.

Absolute tracer recovery from Child Z to Child Y is higher than the recovery from Child Y to Child Z. This suggests Child Z fractures had upward height growth into the landing zone of Child Y. This could potentially be a result of the completion order, as Child Z injected fluid and tracer that could have displaced Child Y tracer that would otherwise have been produced had it been completed last.

Case Study I focused on matching near field tracer recovery, with absolute tracer recoveries vs. time higher than those observed from far field recovery wells in Case Study II. Yet this focus in Case Study I resulted in estimation of horizontal vs. vertical toughness that is corroborated by both the near and far field tracer recoveries calculated in Case Study II. In both Case Study I and II, hydraulic fractures explained the transport of tracers without incorporating the presence of natural fractures or faults.

Case Study III: Applied Learnings, Different Region

The next case study is located in Region 1, across the Midland Basin from Region 2. While absolute model parameters such as pressure, distribution of facies, and stress magnitude differ between the two regions, the workflow to derive these input parameters was the same. Learnings regarding toughness from Case Studies I and II were incorporated into the development of the Case Study III model in Region 2. The Region 2 model was history matched with the assistance of geochemical production allocation diagnostic data shared in the companion paper by Albrecht et al. (2022). A new simulation model was then built to test model validity surrounding toughness using recently acquired tracer test data available in the vicinity. The gun barrel view and sequence of horizontal well development across multiple landing zones is depicted in **Fig. 18**.

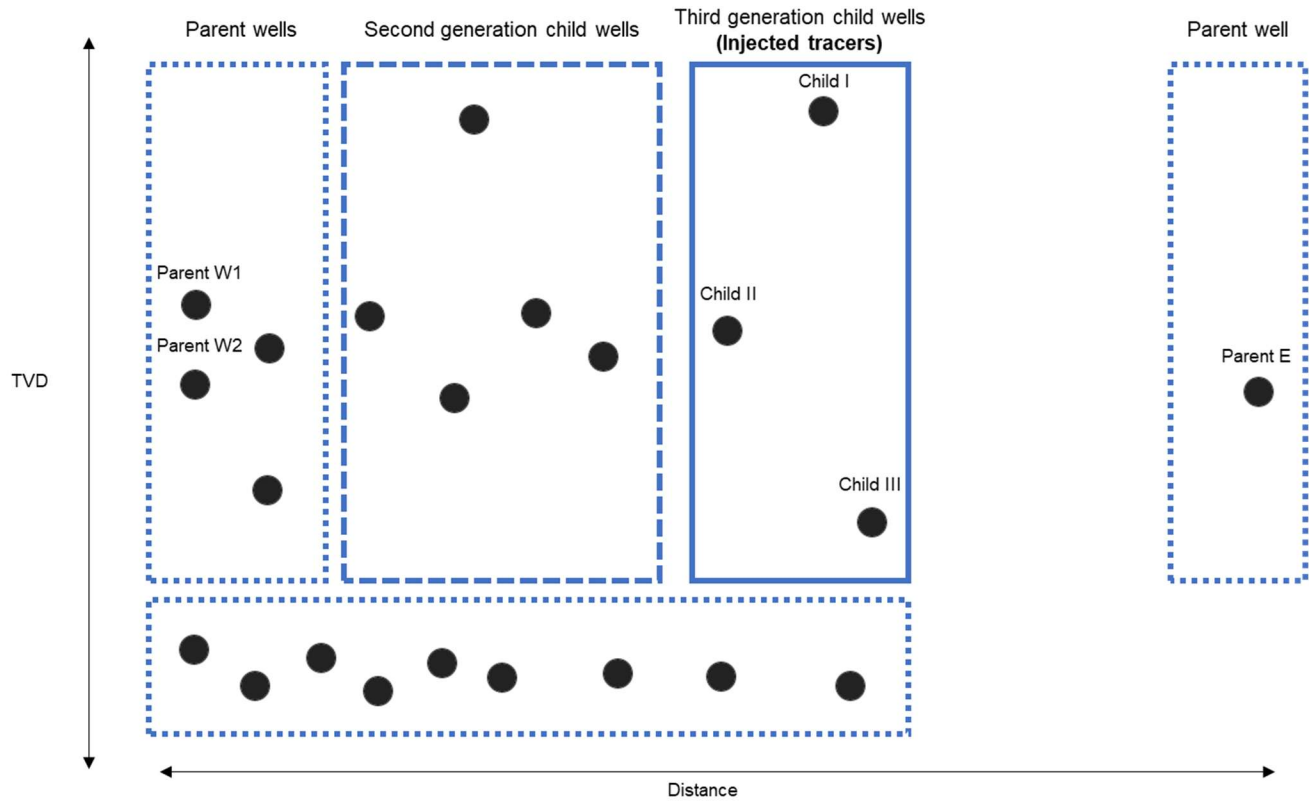

Fig. 18—Layout of parent, child, and traced wells in Case Study III, Region 1.

Unique water and oil tracers were injected into five completion stages in Child I, Child II, and Child III, which are all third-generation wells in development sequencing. Substantial amounts of tracer from all three traced wells were recovered in the second-generation child wells, all of which were restarted prior to the startup of the actual traced wells.

In total, 22 wells were included in this tracer study. Applying Eq. 4 to this well layout yields an additional 132 potential history matching parameters due to the injection of tracers. A simplified model was built consisting of only wells Parent E, W1, W2 and the three traced third generation child wells to determine if the toughness assumptions in Region 1 were applicable in Region 2.

Because not all wells producing tracer were included in the model, actual boundary conditions of Child I, II, III, Parent W1 and W2 are not honored. The well closest to honoring actual boundary conditions was Parent E, which remained flowing during the injection of tracers in Child I, II, and III. Parent E actual and modeled water production also increased because of communication with the completions in Child I, II and III.

Parent E was completed in 2014 and used a low number of completion clusters, resulting in a low number of modeled hydraulic fractures. One of the uncertainties in these case studies is the distance unique planar fractures connect versus continue to propagate in parallel to a neighboring fracture. Case Study III examined a sensitivity focusing on the distance of fracture connection specified within the model, with hydraulic fractures from different wells connecting at distances if propagating within 2.4ft of each other, or within 3.6ft. The lower the distance, the more resulting unique hydraulic fractures are generated in the model. Results of this sensitivity comparing the actual amounts of tracer recovered vs. the simulation model from Parent E is shown in **Fig. 19**.

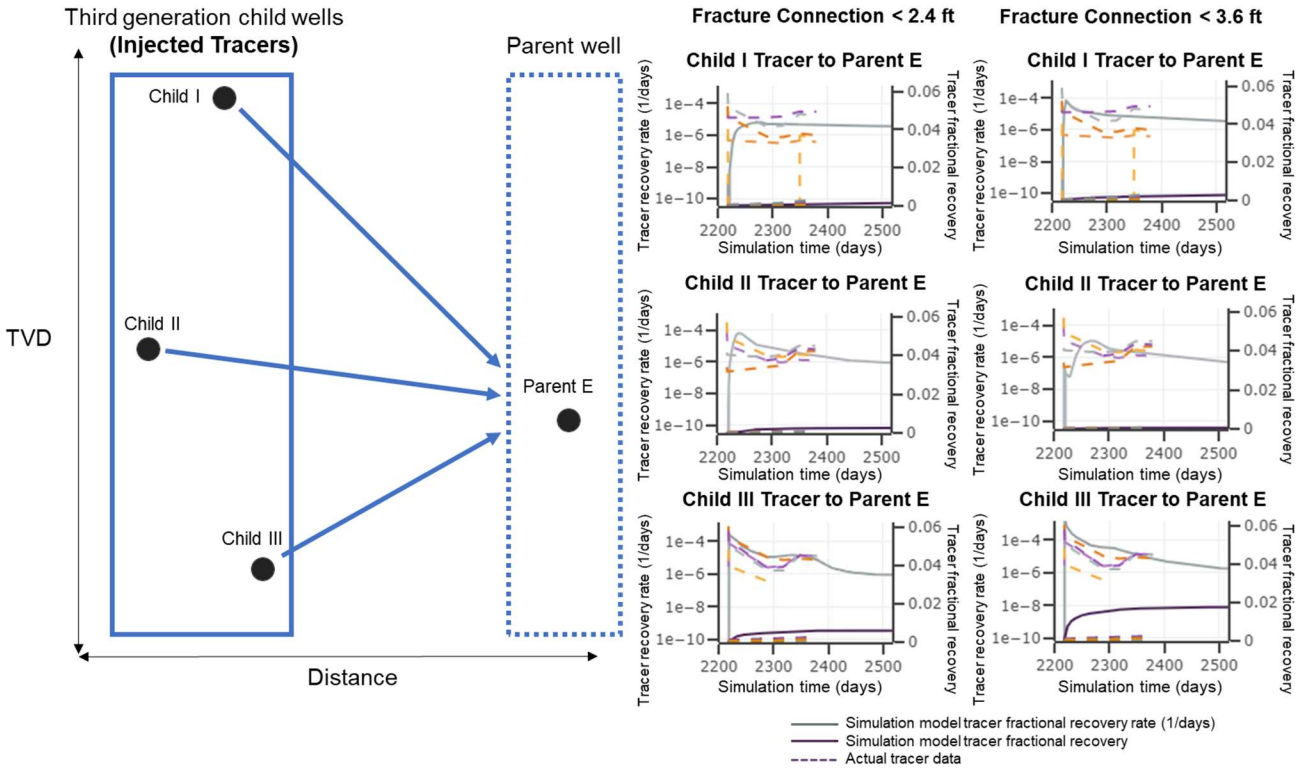

Fig. 19—Child I, II, III water tracer rate and recovery from Parent E varying model fracture connection distances, Case Study III, Region 1.

The modeled tracer results most closely match the actual data for fracture connection distances less than 2.4 ft. This distance is consistent with the hydraulic fracture occurrence on the order of 500 fractures per 1000 ft of core noted in the HFTS-2 slant core offsetting multi-well development in the Delaware Basin (Gale et al., 2021).

The mechanism of tracer transport through the hydraulic fractures in Case Study III is one of reopening existing hydraulic fractures. **Fig. 20** shows several property views of the hydraulic fractures that initiated from Parent E at the start of Child III tracer production. While other fractures are modeled in the simulation, only the fractures that initiated from Parent E (including collision and growth caused by Parent W2) are shown in Fig. 20.

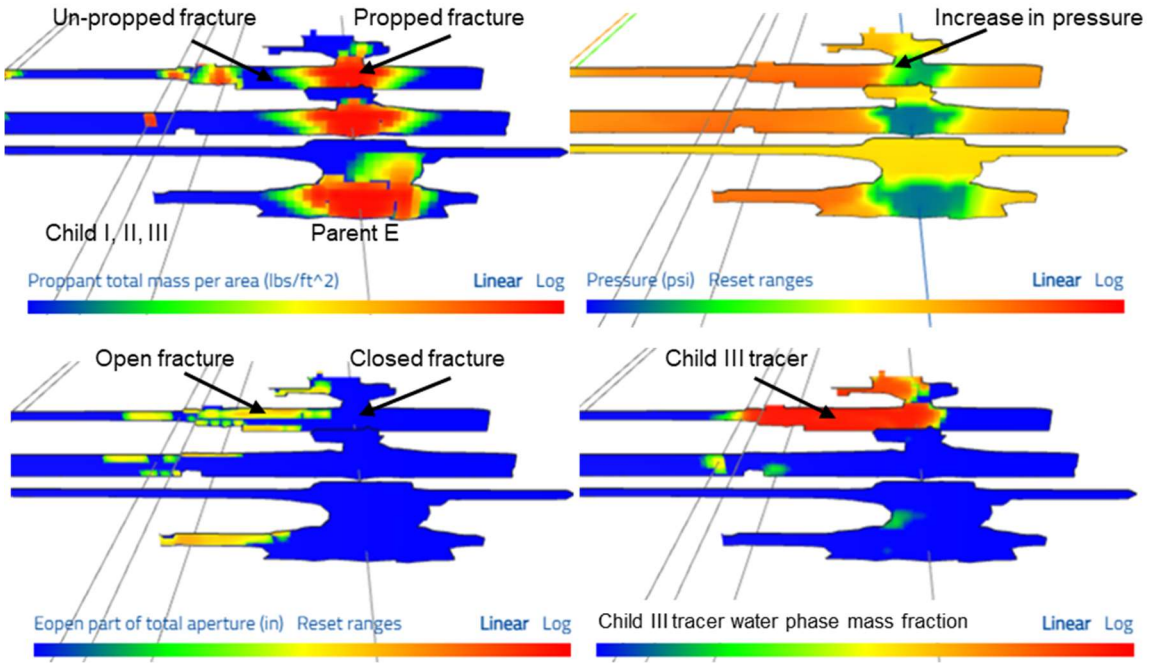

Fig. 20—Fractures originating from well Parent E at time of Child III tracer production.

The upper left view shows the location of proppant in Parent E fractures, with blue indicating unpropped fractures. The upper right plot shows the pressure increase within the fracture as the water from Child III travels through the Parent E fracture. The lower left plot shows the status of the Parent E fracture, reopened in yellow and orange, and closed in blue. Finally, the lower right plot shows the water tracer from Child III flowing into the Parent E fracture. The open status of the fracture means that the hydraulic fracture has been reopened due to the injection into Child III. Hydraulic fracture reopening is the mechanism of tracer transport in the communication between Parent E and Child III in the simulation model. **Fig. 21** shows this same view three years later during production within the simulation model.

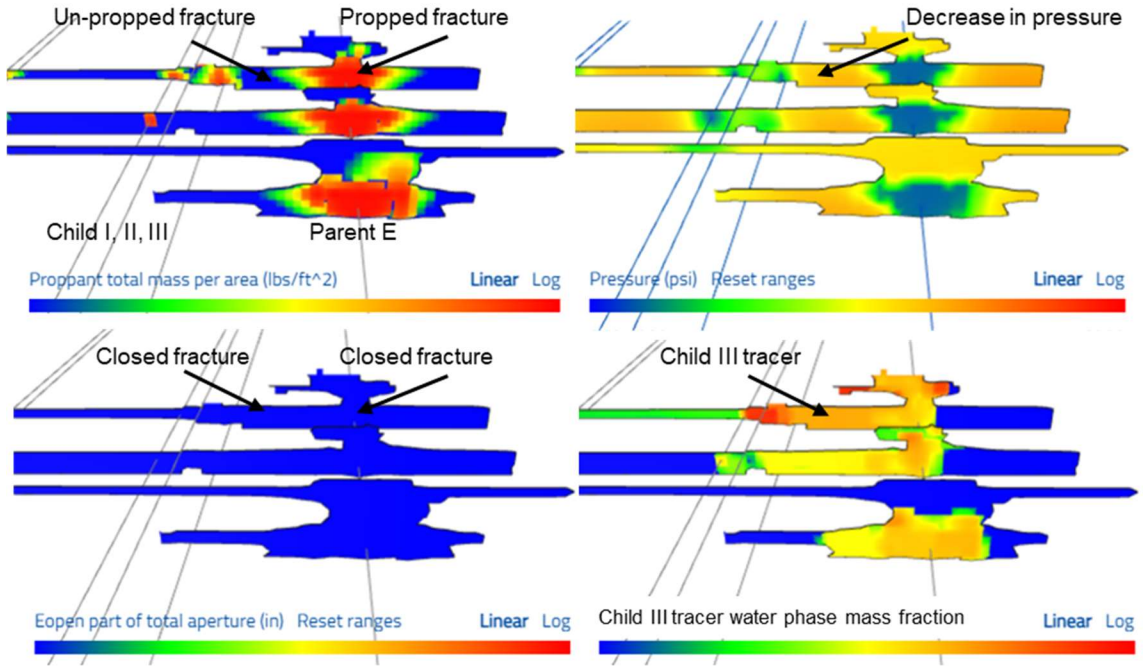

Fig. 21—Fractures originating from well Parent E three years after Child III tracer was injected.

The black arrows in Fig. 21 show a decrease in pressure in the unpropped, closed fractures and a decrease in Child III tracer. This suggests that tracer in the model is still being transported in fractures that are unpropped. While these are simulator results based on model inputs and settings, and three years have not actually elapsed since this tracer study began, it illustrates the potential contribution unpropped fractures may play. The match or mismatch between actual and modeled tracer production over time will indicate whether these settings allowing for unpropped fracture contribution are correct or require adjustment.

Case Study III presented many challenges around planning, execution, and interpretation of data. The cost of a tracer study is based on the mass of tracer used and number of samples analyzed over time. The cost of tracer studies scales with the number of well samples analyzed. Balancing the cost of a study including 22 wells sampled over a longer period required taking fewer early time samples, resulting in lower resolution data early time. Fewer early time samples meant tracer recovery calculations are less confident in certain study wells, just as production data missing early time makes cumulative voidage unknown. However, the tracer recovery rate data at the same modeled time suggest good agreement in both timing and order of magnitude, suggesting modeled toughness inputs are appropriate.

Additionally, planning and executing around the actual sampling of 22 wells proved difficult in Case Study III. Case Study II consisted of two producing offset wells requiring sampling when tracer was injected, with a later addition of three parent wells for a total of five parent wells requiring samples. Further, the child wells including the two wells with tracer injected all started production at the same time, allowing for a consistent sampling schedule for field personnel. In contrast, the parent and second-generation child wells in Case Study III were more numerous, 19 in total. Some of these 19 offset wells were considered deferred production and were restarted at different times. This resulted in a complicated sampling schedule to execute upon restart.

Tracer Amount and Selection

While the theory section introduced the necessary qualities of conservative phase tracers, the reality is that many of the tracers in use may not be ideal for the purpose of implementing quantitative analysis. **Fig. 22** shows the complete tracer dataset from Well A tracer produced from Well A in Case Study I. This includes tracer recovery rates that span an order of magnitude, and tracer recoveries that range from zero to 10% in the first six months of production. All tracers were injected with the same completion design, meaning differences in tracer results must be explained.

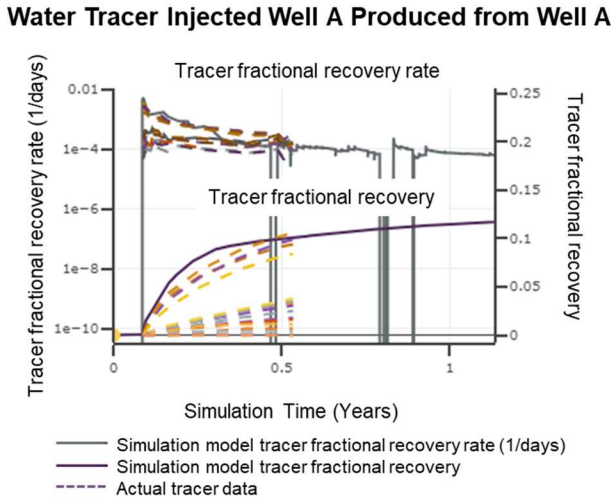

Fig. 22—Complete set of tracer results from Well A, including results spanning an order of magnitude.

Table 3 contains the raw tracer concentration data produced from Well A of its own water tracer in Case Study I. This sampling occurred over six months and began at the start of production.

Tracer Injected (g)	4831	5079	4748	4676	4666	4605	3386	3481	3528	3623	3765	1255	1492	1302	1208	521
% Injected	9%	10%	9%	9%	9%	9%	6%	7%	7%	7%	7%	2%	3%	2%	2%	1%
Sample Date	CFT 2000	CFT 1700	CFT 1200	CFT 1300	CFT 1100	CFT 1000	CFT 2100	CFT 2400	CFT 2200	CFT 2500	CFT 1600	CFT 10800	CFT 4000	CFT 10850	CFT 10650	CFT 10250
1/11/17 9:00	1.2	1.5	1.9	32.3	24.5	24.2	10.8	1.5	0.7	0.0	0.3	0.0	0.0	0.0	0.0	0.0
1/12/17 11:00	1.6	2.4	2.0	29.0	22.0	24.0	10.7	1.9	0.8	0.0	0.5	0.0	0.0	0.0	0.3	0.0
1/13/17 16:00	2.2	3.7	2.1	27.0	20.7	22.7	11.0	2.8	0.9	0.5	1.0	0.0	0.0	0.0	0.3	0.0
1/14/17 1:00	2.3	3.5	2.0	24.6	18.9	22.3	10.4	2.7	1.0	0.6	1.3	0.0	0.3	0.0	0.4	0.0
1/15/17 13:00	2.2	3.8	0.9	17.2	15.0	17.1	8.3	2.8	1.0	1.0	2.4	0.0	0.3	0.3	0.0	0.0
1/17/17 13:00	1.9	3.5	1.1	15.0	13.0	15.9	7.3	2.2	0.9	1.4	2.5	0.0	0.3	0.3	0.0	0.0
1/19/17 13:00	1.9	3.5	1.0	14.5	12.8	15.7	7.2	2.5	1.0	1.9	3.0	0.0	0.3	0.4	0.0	0.0
1/21/17 13:00	2.1	3.9	1.2	12.5	12.0	14.9	7.3	2.2	1.1	3.2	3.7	0.0	0.5	0.7	0.0	0.0
1/23/17 13:00	1.8	3.5	1.6	11.9	11.6	14.0	6.9	2.0	1.0	3.1	3.6	0.0	0.4	0.5	0.0	0.0
1/27/17 13:00	1.9	3.1	1.4	10.0	10.5	13.0	6.3	2.1	1.0	2.9	3.4	0.0	0.3	0.5	0.0	0.0
1/31/17 13:00	1.9	3.0	1.6	9.1	9.3	11.7	5.6	1.7	0.9	1.9	2.8	0.0	0.3	0.4	0.0	0.0
2/7/17 13:00	1.5	2.8	2.4	7.6	8.3	8.4	5.2	1.7	1.2	1.7	1.6	0.0	0.3	0.5	0.0	0.0
3/14/17 10:00	1.0	2.4	1.6	4.8	5.1	5.1	3.4	1.2	0.7	1.7	1.9	0.4	0.0	0.3	0.0	0.0
4/25/17 10:00	0.8	1.5	1.3	2.8	3.8	3.7	2.4	1.0	0.6	1.2	1.4	0.0	0.0	0.0	0.0	0.0
5/3/17 11:07	0.7	1.2	1.1	2.9	3.4	3.1	2.0	0.8	0.5	1.1	1.2	0.0	0.0	0.0	0.0	0.0
6/6/17 13:00	1.0	1.9	1.5	2.7	3.2	3.1	2.1	1.6	0.7	2.2	1.8	0.0	0.0	0.0	0.0	0.0
6/13/17 0:00	0.7	1.4	1.1	2.3	2.6	2.9	1.7	1.2	0.5	1.3	1.6	0.0	0.0	0.0	0.0	0.0
6/23/17 0:00	0.7	1.4	1.0	1.8	2.5	3.0	1.6	1.0	0.4	1.2	1.8	0.0	0.0	0.0	0.0	0.0

Table 3—Raw tracer concentration results from Well A water tracer. Note the low to zero concentrations and amount injected.

Note how concentrations of many of these tracers are low or zero and approaching the detectable concentration limit at only six months into the study. This results in large differences in tracer recovery rate observed in Fig. 22, and subsequently the differences in calculated recovery. Upon further investigation, it was noted that some of these stages with lower calculated recovery also used a mass of tracer injected that is low, approximately 1 kg (**Fig. 23**). Tracers with the highest fraction of tracer recovered tend to have a higher overall mass injected.

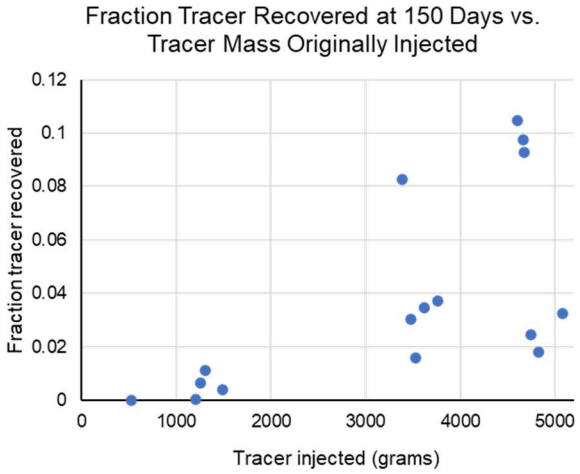

Fig. 23—Observed relationship between tracer recovered and total mass of tracer injected.

The remaining tracers with 3-5 kg injected with low recoveries may be indicative that not all tracers used in this study are ideal conservative tracers, and therefore may be unsuitable for quantitative tracer analysis. This may be due to partitioning of water tracers into the oil phase, resulting in unmeasured amounts of tracer recovery.

These findings suggest that it is critical to inject a sufficiently large mass of tracer in order to allow for prolonged sampling of tracers in a study. Furthermore, non-ideal tracers must be identified prior to executing a tracer study. One way to determine tracer suitability for mass balance purposes is to inject all potential tracers into the same completion stage and measure each tracer concentration. Different tracer

recovery rates will indicate tracer suitability. This testing was not done prior to executing the case studies shared in this paper but assumed the highest tracer recovery rate presented the most reliable data.

Tracer Study Design Considerations

This section discusses learnings around tracer study design, field execution, and use within reservoir simulation.

Number of Wells Included in Studies

1. Design tracer studies with a manageable number of wells and tracers. This is advantageous for both execution in the field and building and running simulation models.
2. Design studies that will allow for both near and far field understanding through the placement of offset wells. Simulation model run time scales with the number of tracers used in simulations as well as the number of wells. Starting with a simple two well tracer model discussed in Case Study I allowed much faster learning than building complicated 8+ well models. Case Study II demonstrated building and matching a 14 well model is possible, but Case Study I with only two wells was sufficient for characterizing hydraulic fracture and production mechanisms.

Injection, Sampling, and Timing Considerations

1. Inject enough mass of tracer to allow for long-term sampling above the detection limit. Document injected mass of tracer.
2. When injecting tracers, consider the effect of the order completed. In Case Study II, traced wells Child Y and Child Z were deliberately completed last so the tracer was not transported by the completion fluids of other child wells further east.
3. At the end of a completion stage, flush volumes are injected into a well to displace all completion fluid, tracer, and proppant into the stage. After injection of all stages is complete, the plugs of each stage are drilled out and circulation occurs. No consideration of the effects of drill out and this circulation are accounted for in the model, just as tracer samples in these case studies do not include this time period.
4. Frequent early time sampling of tracer is critical, both from capturing samples from all offset wells upon well startup to capturing parent-child interactions during tracer injection. While gaps in early time sampling leads to errors in the tracer recovery calculations, any sample taken in the future can always be accurately compared against tracer recovery rate alone. Late time sampling past a typical six-month schedule on the order of years should also be designed for, including the addition of samples from new infill wells upon startup. Long term tracer data may provide information about the contribution and properties of unpropped fractures.
5. Plan to sample all wells within the distance where increased water production is observed after the offset well completion.
6. Collect samples in glass bottles, not plastic, in order to avoid tracer loss or gain.
7. Every time an infill well is completed, the boundary conditions in the field and the model permanently change. Design studies around maximizing the sample time window before infill wells are completed. Take final samples before infill wells are completed.

Stakeholders

1. A successful tracer study requires coordination and communication among engineers utilizing this data, service companies, field personnel, development plans and potentially outside operators. Collaboration should occur in the initial planning phases as well as throughout execution of tracer injection and sampling.

Discussion

When quantitative tracer analysis was first applied to these simulation models, other diagnostic data available was limited to observations of fracture interactions such as increased water production from producing wells offsetting completing wells. The tracer case studies suggested that the hydraulic fractures have very substantial length and height. Since then, geochemical production allocations (Albrecht et al. 2022) and DAS data were gathered, and both were compared with modeled results. This new data has confirmed the tracer results regarding fracture geometry.

Tracer recovery must be considered in the context of time. 1% tracer recovery may seem like a low absolute value, but when that amount is recovered from an offset well three months into production, what are the implications for tracer recovery over 240 months or more of production? **Fig. 24** compares the tracer recoveries of Well A from Case Study I with Child Z from Case Study II, as both have a similar landing zone. In the first 90 days of production, Well A recovered between 5-10% of its own water tracer. Well A had little bounding from other wells at the time, only Well B beneath. This contrasts with Child Z from Case Study II, which was laterally and vertically bounded by 13 other wells, 11 of which produced its water tracer. Child Z only recovered 2% of its own tracer during that time, and vertically offset well Child Y recovered approximately 1% of Child Z's tracer. The total amount of Child Z tracer recovered by all the Case Study II wells in the first 90 days was approximately 5%.

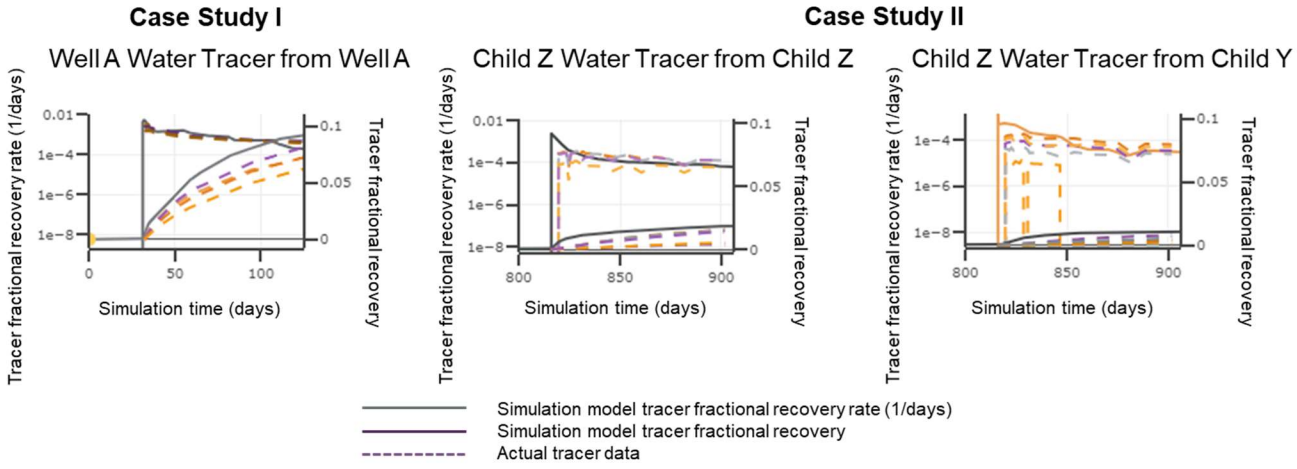

Fig. 24—Comparison between laterally unbounded Well A and bounded Child Z tracer recoveries.

Just as the tracer recovery of Well A tracer from Well A is higher than the recovery of Child Z tracer from Child Z, so too is the estimated ultimate recovery. This means that tracers, much like production, reveal potential long-term implications with respect to well spacing.

Case Study I only had six months of tracer data available. Well A recovered 10% of its own tracer during this time. When the simulation model was run for a total of 30 years, over 20% of the tracer was recovered (**Fig. 25**).

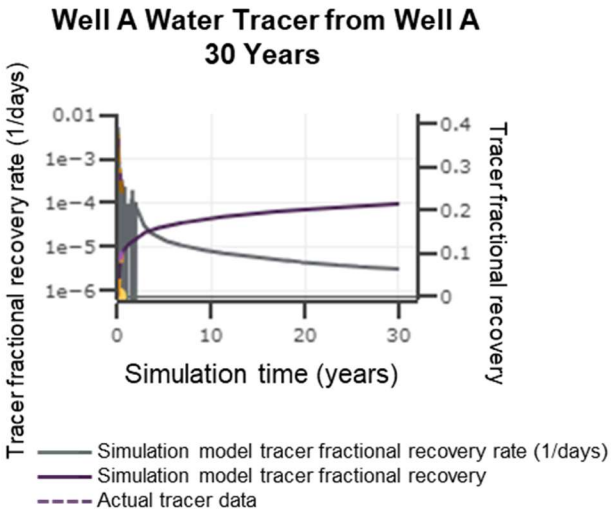

Fig. 25—Simulation model predication of Well A tracer recovery from Well A, thirty years into production.

This 20% of Well A tracer recovered over time is pictured in **Fig. 26**. Well A tracer water phase mass fraction is shown at three different timesteps alongside proppant total volume fraction (logarithmic scale) within the fractures in the upper left portion of Fig. 26.

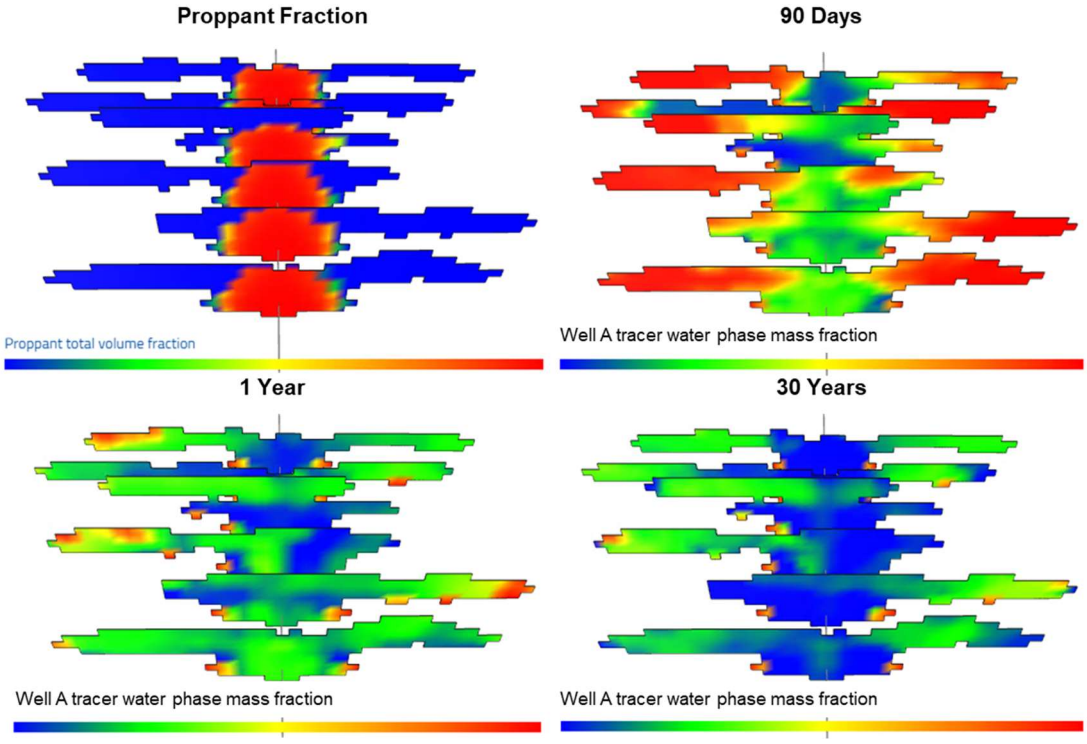

Fig. 26—Simulation model of Case Study I Well A tracer fraction over thirty years. Note location of proppant relative to tracer fraction.

In the model, tracer concentration rapidly changed over the first year of production, with less change observed over the remaining 29 years. Most of the change is concentrated in the location of proppant. Some change is observed in the unpropped fractures within the model, suggesting some degree of contribution from unpropped fractures.

One known limitation of our current tracer studies is that we do not have long term (~30 yrs) produced tracer data which would help us better understand how both propped and unpropped fractures produce. Continual infilling of the Permian Basin results in constantly changing boundary conditions making this an increasingly complex challenge over time.

All models encountered fracture propagation after injection of completion fluids and tracers ceased, a consequence of viscous pressure drop along the fracture during injection (**Fig. 27**). This is consistent with observations from DAS data in vertical offset monitoring wells of fracture propagation after hydraulic fracture injection ceases in the Delaware Basin (Ugueto et al. 2021).

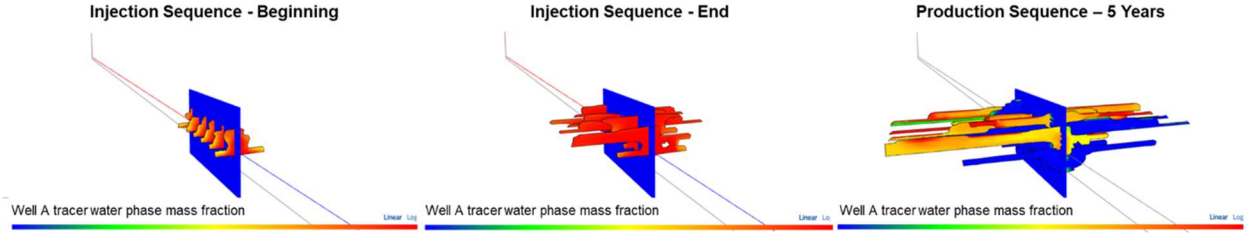

Fig. 27—Hydraulic fracture propagation with tracers, before and after stimulation ceases.

History matches were achieved with planar fracture geometries, which is consistent with recent published core-through and fiber optic diagnostics in the Midland Basin and other shale plays (Gale et al. 2018; Shahri et al. 2021; Ugueto et al. 2021). An example of the simulation model for the wells in Case Study I is shown in Fig. 27, visually demonstrating the planar fracture geometries. While natural fractures have been observed in core-through studies (Gale et al. 2019), the simulation models shared in these case studies did not contain any faults or natural fractures and were not required to match production rates or actual tracer data.

Other Model Considerations

While we do account for variability in formation properties across the basin, we have found that high-level model parameters (such as fracture toughness) calibrated in one area can be used consistently across the basin. Trends in vertical variability in model inputs such as hydrocarbon saturation, pore pressure, and geomechanical inputs such as minimum horizontal stress and toughness are consistently honored in all models across the Midland Basin case study wells. Models in both Region 1 and 2 use similar permeability relative to oil in the matrix. Despite differences in absolute values of static model properties, the case study wells in Regions 1 and 2 encounter similar production behavior based on diagnostic tracer data.

Model inputs and settings impacting the results of tracers include leakoff into the matrix, fracture conductivity and relative permeability within the fracture mesh, and how hydraulic fractures do or do not connect at far field. Limiting water leakoff from the hydraulic fracture mesh into the matrix resulted in better history matches and avoided issues with numerical dispersion or implementation of local grid refinement. While we know some leakoff occurs, the key learning was that leakoff distance away from the hydraulic fracture into the matrix is minimal and tracer stays near the hydraulic fractures until production begins. This understanding was also important toward achieving history matches with respect to water production rates and overall watercut, as well as identifying sources of additional formation water beyond injected completion fluids. The conductivity of the hydraulic fracture mesh is a product of the proppant properties and its location within the fractures as a result of injection.

In the proppant pack, relative permeability curves with low Corey exponents were used. In mechanically open fractures, an ‘X’ curve was required when using hydrocarbon tracers as oil tracer injection results in very low oil saturations within the fracture mesh. Sensitivities around hydraulic fracture connection distances suggested hydraulic fractures tend to connect far field at distances around 3 ft. This was

discussed in Case Study III and is consistent with HFTS-2 learnings on observed hydraulic fracture occurrence vs. distance through core (Gale et al. 2021).

An extension of this work is to use both models and actual data and apply additional quantitative tracer analysis techniques to unconventional tracer studies. This includes deriving flow and storage capacity, swept volume, etc. from tracer data using methods outlined in papers by Shook (2003) and Shook et al. (2009).

Conclusions

1. This paper demonstrates the usefulness of quantitative tracer analysis as a means of understanding hydraulic fracture geometry and production behavior.
2. Tracer data proved useful in constraining model inputs that control fracture geometry, specifically toughness, toughness anisotropy, and the propensity for fractures to collide versus grow past each other.
3. Models constrained through the quantitative analysis of tracer data are corroborated by other diagnostic tools such as DAS and geochemical production analysis.
4. History matches constrained using tracers result in higher confidence models than models history matched solely using pressure and rate data, and allow for more robust sensitivities to determine the optimum well spacing and completion design for an asset.

References

Albrecht, Magdalene, Borchardt, Shannon, and Mark McClure. “Using Geochemical Production Allocation to Calibrate Hydraulic Fracture and Reservoir Simulation Models: A Permian Basin Case Study.” Paper presented at the SPE/AAPG/SEG Unconventional Resources Technology Conference, Houston, Texas, USA, June 2022. doi: https://doi.org/10.15530/urtec-2022-3724091

Ali, E., Chatzichristos, C., Aurdal, T., and J. Muller. "Tracer Simulation to Improve the Reservoir Model in the Snorre Field." Paper presented at the International Oil and Gas Conference and Exhibition in China, Beijing, China, November 2000. doi: https://doi.org/10.2118/64796-MS

Brigham, W.E., and Smith, D.H.: “Prediction of Tracer Behaviour in Five-Spot Flow,” paper SPE 1130 presented at the 1965 SPE Production Research Symposium, Tulsa, May 3-4.

Danckwerts, P.V., 1953, “Continuous Flow Systems, Distribution of Residence Times,” *Chemical Engineering Science*, Vol. 2, No. 1, pp.1-18.

Dontsov, Egor, Christopher Hewson, and Mark McClure. 2022. A new crack propagation algorithm that enables accurate simulation of propagation across thin layers in a practical field-scale fracturing model. Paper SPE 209146-MS presented at the SPE Hydraulic Fracturing Technology Conference, The Woodlands, TX.

Du, Yuqi, and Linhua Guan. "Interwell Tracer Tests: Lessons Learnted from Past Field Studies." Paper presented at the SPE Asia Pacific Oil and Gas Conference and Exhibition, Jakarta, Indonesia, April 2005. doi: https://doi.org/10.2118/93140-MS

Fowler, Garrett , McClure, Mark , and Craig Cipolla. "A Utica Case Study: The Impact of Permeability Estimates on History Matching, Fracture Length, and Well Spacing." Paper presented at the SPE Annual Technical Conference and Exhibition, Calgary, Alberta, Canada, September 2019. doi: https://doi.org/10.2118/195980-MS

Gaibor, A. and R.. Rodriguez. "Reservoir Tracer Application to Validate a Numerical Simulation Model: An Historical Case." Paper presented at the SPE Latin American and Caribbean Petroleum Engineering Conference, Quito, Ecuador, November 2015. doi: https://doi.org/10.2118/177210-MS

Gale, Julia F. W., Elliott, Sara J., and Stephen E. Laubach. "Hydraulic Fractures in Core From Stimulated Reservoirs: Core Fracture Description of HFTS Slant Core, Midland Basin, West Texas." Paper presented at the SPE/AAPG/SEG Unconventional Resources Technology Conference, Houston, Texas, USA, July 2018. doi: https://doi.org/10.15530/URTEC-2018-2902624

Gale, Julia, Elliott, Sara, Li, John Z., and Stephen Laubach. "Natural Fracture Characterization in the Wolfcamp Formation at the Hydraulic Fracture Test Site (HFTS), Midland Basin, Texas." Paper presented at the SPE/AAPG/SEG Unconventional Resources Technology Conference, Denver, Colorado, USA, July 2019. doi: https://doi.org/10.15530/urtec-2019-644

Gale, J. F. W., Elliott, S. J., Rysak, B. G., Ginn, C. L., Zhang, N., Myers, R. D., and S. E. Laubach. "Fracture Description of the HFTS-2 Slant Core, Delaware Basin, West Texas." Paper presented at the SPE/AAPG/SEG Unconventional Resources Technology Conference, Houston, Texas, USA, July 2021. doi: https://doi.org/10.15530/urtec-2021-5175

McClure, M., C. Kang, S. Medam, C. Hewson, and E. Dontsov. 2022 ResFrac Technical Writeup. [Online]. Available: https://arxiv.org/abs/1804.02092.

Shahri, Mojtaba , Tucker, Andrew , Rice, Craig , Lathrop, Zach , Ratcliff, Dave , McClure, Mark , and Garrett Fowler. "High Fidelity Fibre-Optic Observations and Resultant Fracture Modeling in Support of Planarity." Paper presented at the SPE Hydraulic Fracturing Technology Conference and Exhibition, Virtual, May 2021. doi: https://doi.org/10.2118/204172-MS

Shook, G. Michael, 2003. “A Simple, Fast Method of Estimating Fractured Reservoir Geometry from Tracer Tests,” *Geothermal Resources Council Transactions*, Vol. 27, October.

Shook, G. Michael, S. L. Ansley and A. Wylie, 2004. “Tracers and Tracer Testing: Design, Implementation, and Interpretation Methods,” INEEL 03-01466, January.

Shook, G. Michael, 2005. “A Systematic Method for Tracer Test Analysis: An Example Using Beowawe Tracer Data,” SGP-TR-176, Proceedings, Thirtieth Workshop on Geothermal Reservoir Engineering. Stanford University, Stanford, California, January 31-February 2.

Shook, G. Michael, Pope, Gary Arnold, and Kazuhiro Asakawa. "Determining Reservoir Properties and Flood Performance From Tracer Test Analysis." Paper presented at the SPE Annual Technical Conference and Exhibition, New Orleans, Louisiana, October 2009. doi: https://doi.org/10.2118/124614-MS

Ugueto, Gustavo A., Wojtaszek, Magdalena, Huckabee, Paul T., Savitski, Alexei A., Guzik, Artur, Jin, Ge, Chavarria, J. Andres, and Kyle Haustveit. "An Integrated View of Hydraulic Induced Fracture Geometry in Hydraulic Fracture Test Site 2." Paper presented at the SPE/AAPG/SEG Unconventional Resources Technology Conference, Houston, Texas, USA, July 2021. doi: https://doi.org/10.15530/urtec-2021-5396